Flexural Behavior of Built-Up Cold-formed Steel Channel Section Strengthened with Oriented Strand Board

Mohd Syahrul Hisyam Mohd Sani[1,*], Haslin Idayu Amaruddin[1], Wan Mohd Nazri Wan Abdul Rahman[2], Fadhluhartini Muftah[1]

[1]School of Civil Engineering, College of Engineering, Universiti Teknologi MARA (UITM) Pahang Branch, Pahang, Malaysia

[2]Faculty of Applied Science, Universiti Teknologi MARA (UiTM) Pahang Branch, Pahang, Malaysia

Received 09 January 2023; received in revised form 22 March 2023; accepted 26 March 2023

DOI: https://doi.org/10.46604/ijeti.2023.11380

Abstract

The objective of the study is to determine the flexural behavior of the built-up cold-formed steel (CFS) channel section strengthened with an oriented strand board (OSB) in the three-point bending experiment. CFS with a variety of shapes and grades is classified as a steel-based material and exposed to buckling failure when subjected to compression or flexural load. Thus, the CFS channel section with 100 mm of the web, 50 mm of the flange, 12 mm of the lip, and 1.55 mm of thickness has been selected. Then, the built-up CFS channel section is designed by filling with an OSB between the gap of each section. Channel, face-to-face built-up, and back-to-back built-up CFS sections are three types of tested specimens. From the result and discussion, the specimen with back-to-back built-up CFS section is recognized to sustain the ultimate load with the highest value when compared with other specimens.

Keywords: cold-formed steel, flexural behavior, oriented strand board, channel section, built-up section

1. Introduction

Cold-formed steel (CFS) is a steel-based material created at room temperature using steel sheets bent and rolled for structural or non-structural purposes. Another example of a steel-based material is hot-rolled steel which is different in the method of manufacturing and uses a high-technology machine with a lot of energy consumption. CFS is formed through pressing, bending, and rolling at normal temperatures and is broadly used as a structural and non-structural component. Hot-rolled steel is classified as a high-cost material, heavyweight with a high maintenance cost, and is different from CFS which shows a lot of advantages such as cost-effectiveness, lightweight, fast erection or installation, ease of transport and handle, corrosion resistance, etc.

Nowadays, many researchers are studying and discussing the CFS to swift hot-rolled steel as a structural component such as beams and columns. In the construction industry, the CFS is often used for the channel, angle, zed, and hat sections, but it may also be produced in a vast array of shapes, cross-sectional areas, and thicknesses. This well-liked section is categorized as an open section, which is typical of an asymmetrical section and is vulnerable to failures. If no serious action is taken, it may result in collapse and structural integrity problems. In residential houses or buildings, CFS is employed as an interior wall panel, storage rack panel, and roof truss system.

* Corresponding author. E-mail address: msyahrul210@uitm.edu.my

English language proofreader: Hsin-Te Hsieh

As mentioned before, structural integrity is becoming a critical issue if the section is proposed for the structural element because the CFS material available in the market is an open and unsymmetrical section. Normally, CFS with an open section and slender is often vulnerable to failure owing to buckling or instability circumstances, which can fall into one or a combination of four categories for example local, distortional, lateral, and global buckling. Local and distortional buckling is deformed on the flange and web element but the corner of the flange and web element is still in position. However, as illustrated in Fig. 1, the overall section is moved and displaced to a different location due to lateral and global buckling. This failure is a critical issue that must be solved before it becomes more serious and influences the overall structure. Additionally, the slenderness of the CFS structural element enhances the susceptibility to instability failure.

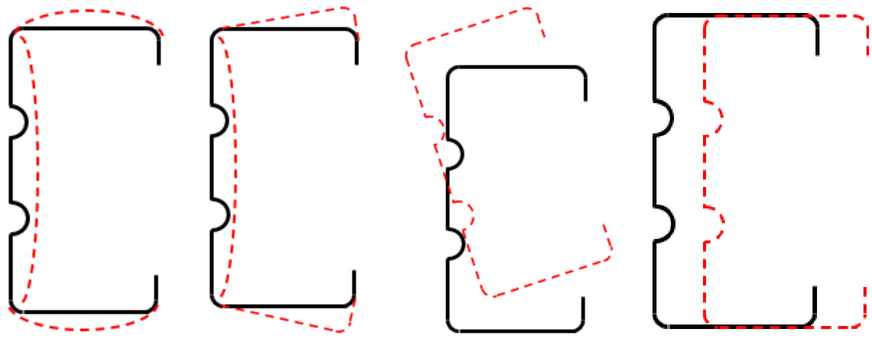

Fig. 1 The type of failure of the buckling that occurred in the CFS section [1]

To solve the problem, CFS is studied to form or to create by using several techniques or methods such as intermittently stiffening, externally stiffening, adoption of corrugated web profiles, adoption of composite sections, etc. Usually, CFS is studied to propose becoming a built-up section with a closed section or symmetrical section which is known as intermittently or externally stiffening techniques. There are a lot of studies that focused on intermittently stiffening techniques such as Selvaraj and Madhavan [2], Dar et al. [3] and Guzman et al. [4], and carried out on external stiffening techniques such as Anbarasu et al. [5]. There are two basics of the built-up CFS section with simple fabrication which is conducted and focused on in this study consisting of a back-to-back and face-to-face configuration.

Nevertheless, the American Iron and Steel Institute (AISI) has limited the prequalified geometry for the design of the beam which is made by using a configuration of back-to-back built-up sections linked with two CFS channels [2]. Selvaraj and Madhavan [2] have reported that due to the ongoing evolution, the existing design guidelines do not provide particular design techniques for the built-up CFS section. The material that has been incorporated should give more advantages for the overall section, such as being cost-effective and being able to reduce the structural integrity.

2. Cold-Formed Steel Composite Section

CFS is investigated to combine with other materials which is recognized as the adoption of the composite section technique for flexural members and nowadays, becoming more popular. There are a lot of studies conducted on this technique for instance Sifan et al. [6] and Dias et al. [7]. Additionally, the composite is made to be extremely strong, resistant to buckling, seismicity, and fire and it is also capable of lowering manufacturing costs and material costs. Examples of the other materials that have always been discussed in the previous study are concrete and mortar. Concrete and mortar are classified as costly materials, expand CO_2 emission and produce a lot of environmental problems at the quarry site. Kyvelou et al. [8] have mentioned that the structural component with the lightweight condition is suitable for earthquake resistance which reduced the inertia load and is suitable for wind action resistance, especially uplift load. CFS is formed as a built-up section by connecting one section or more sections to other sections by using fasteners such as screws, bolts and nuts, welding, and other innovative jointers.

Due to problems that are involved with concrete or mortar, the other materials, such as timber board or related to boards based on timber, or waste materials such as ash or fiber, are introduced to amalgamate with CFS. The timber board is appropriate to combine with CFS because of its flexibility, safety, stability, and durability. The combination of timber board and CFS is designed and jointed by using adhesive, glue, fastener such as screws, bolts and nuts, and resin. There are a lot of types of timber board such as chipboard or plywood board, medium density fiberboard (MDF) board, particle board, oriented strand board (OSB) board, high-pressure laminate (HPL) board, acrylic board and non-timber board for instance cement board, gypsum board, etc. All boards have their advantages and disadvantages, as also their utilization and suitability.

Many researchers focused on the combination of CFS with timber board for flooring systems and wall-bearing system applications. Some of the studies combined the CFS and timber board such as particle board [9], plywood [9], cross-laminated timber [10], and OSB [8] for flooring systems or wall bearing systems. Only a few studies were on proposed new or innovative sections comprising the CFS with timber or non-timber board into one section, and, no information, guidelines, or standard for designing the section. Lastly, several researchers have studied the newly created section made by CFS with timber, for instance, Awaludin et al. [11] as shown in Fig. 2, Irawati et al. [12], Abou-Rayan et al. [13] as shown in Fig. 3 and CFS with engineered cementitious composite [14] as shown in Fig. 4.

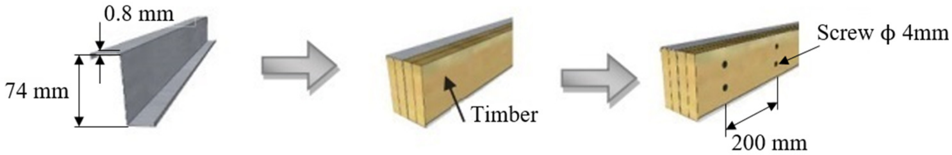

Fig. 2 The production of the composite section with CFS Z-section and timber laminas [11]

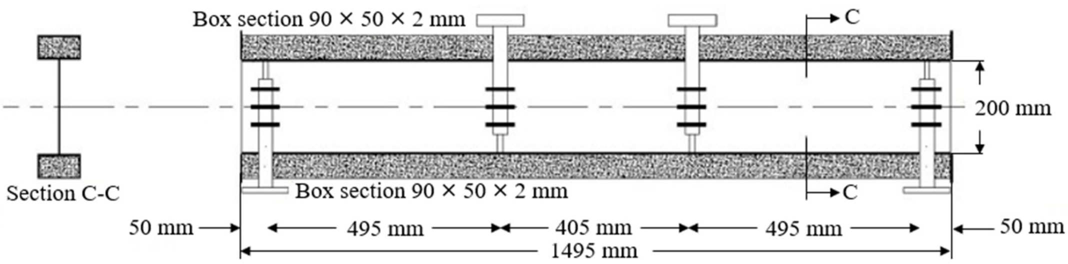

Fig. 3 The CFS I-beam with a strengthened hollow flange on top and bottom with particleboard [13]

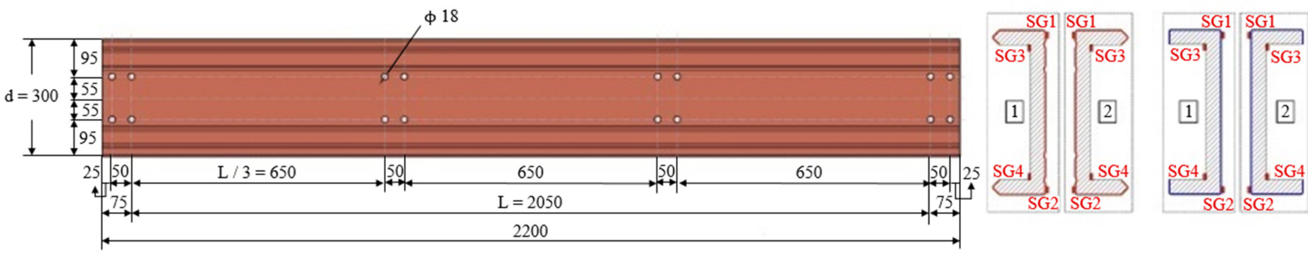

Fig. 4 The CFS channel section combined with engineered cementitious composite [14]

OSB is an engineering timber panel that is popular nowadays as wall sheathing or wall decoration and shaped from a cross-oriented layer of timber strands 8 to 15 cm long and incorporated with adhesives. It makes use of crooked, knotty, and malformed trees that would otherwise go wasted and utilizes the entire tree. The adhesive that is used is from a group of waterproof and heat-resistant types. The timber strands are combined with a waterproof resin, woven into dense mats, and then heated and compressed by pressure to form a great bond. From the process, OSB as building panels that are classified as strong, consistent, and have improved mechanical behavior like high strength and water resistance are the end product. OSB is suitable for usage as roof, wall, and floor sheathing since it is a lightweight, robust, and adaptable timber product. OSB performs and is as strong as plywood in terms of resistance to distortion, bending, and warping.

Additionally, OSB is occasionally utilized as the skin element material for structural insulated panels as well as the web element material for prefabricated I-joists and is used broadly in furniture manufacturing. Normally, OSB is easily obtained from the timber board factory and in the industrial market where the origin of the material is from the Malaysian market or imported from other countries. There are two main objectives of the study including introducing the CFS with an OSB which can minimize the deformation, especially buckling failure. Secondly, to investigate the flexural behavior and determine the failure mode of the built-up CFS strengthened with OSB.

3. Preparation of Material Specimen and Experimental Setup

In this section, the main parts are separated into two components; preparation of material and specimen, and experimental setup. The preparation of material included CFS, built-up CFS, OSB, and built-up CFS with OSB. In addition, the experimental setup is important for the component to determine the material properties of CFS and OSB, and the flexural behavior of the CFS incorporated with OSB.

3.1. Material and specimen preparation

The CFS channel section with a steel grade of G450 and without web stiffener is chosen and section properties obtained from the manufacturer are tabulated in Table 1. The ratio of all elements is examined to ascertain whether the section dimension is suitable as a structural element. Flange element over thickness and flange element over a lipped element has ratios of 32.26 and 4.17, respectively. The ratio between the web element with flange element, web element with thickness, and web element with lipped element is noted as 2.0, 64.52, and 8.33, respectively. Lastly, the lipped element over thickness ratio is reported to obtain 7.74.

To study the section for shifting to the structural component, it is crucial to know the web thickness ratio since it affects the local buckling that occurs when a compression force is applied. According to BS EN 1993-1-1 [15], other factors impacting the various buckling curves include the type of section and web-to-flange element ratio. The lateral-torsional buckling of the CFS channel beam is also influenced by other factors, including the web element-to-flange element ratio, span, residual stress, geometrical imperfections, and material properties [16].

Table 1 The section properties of the CFS channel section

Section dimension and properties			
Notes	Value	Notes	Value
Web, D	100 mm	Flange, F	50 mm
Lipped, L	12 mm	Thickness, t	1.55 mm
Area, A	329 mm2	Yield strength, f_{yf}	450 MPa
Moment of inertia, I_{xx}	0.531×10^6 mm^4	Moment of inertia, I_{yy}	0.109×10^6 mm^4
Section modulus, Z_{xx}	10.625×10^3 mm^3	Section modulus, Z_{yy}	3.237×10^3 mm^3
Radius of gyration, R_x	40.209 mm	Radius of gyration, R_y	18.215 mm
Centroid, X	16.313 mm		
Ratio			
F / t = b / t	32.26	F / L = b / c	4.17
D / F = h / b	2.00	D / t = h / t	64.52
D / L = h / c	8.33	L / t = c / t	7.74

The CFS channel section is clean and clear before being used attached in face-to-face and back-to-back configurations for proposing the built-up CFS section. Besides, the CFS channel section is cut accordingly to the shape of the coupon tensile specimen which is located at the flange and web element in the longitudinal axis. The material properties of CFS are focused on the flat condition which is compared with the factory material properties values and the corner condition is not considered in this study. The coupon tensile specimen is used in determining the material properties of CFS and checking whether the CFS material followed the section properties obtained from the manufacturer that followed BS EN10002-1 [17]. The 50 mm gauge length of the extensometer is located in the middle part of the specimens. For the chemical properties test, CFS is cut into small sizes of 10 mm × 10 mm at any location.

OSB with a size of 1220 mm of width, 2440 mm of length, and 15 mm of thickness is selected and bought from the manufacturer which is easy to attain from the industry market. OSB is cut by referring to CFS for attaching and placing to web element in three layers. In addition, OSB is cut accordingly to the size of testing to determine the physical and mechanical properties such as modulus of rupture (MOR), modulus of elasticity (MOE), internal bond, and thickness swelling.

There are three types of specimens established for calculating the flexural behavior of the built-up CFS channel section strengthened with OSB as tabulated in Table 2. There are proposed three numbers of specimens for every type and another specimen is produced without built-up arrangement and OSB that known as control specimen. The built-up CFS channel section is fastened by using a bolt and nut with the end bolt spacing is 100 mm and middle bolt spacing is 400 mm, for a total length of 600 mm. For the specimen with a length of 400 mm, the end and middle bolt spacing are 100 mm and 200 mm, respectively. The end bolt spacing for both specimens is constant and the use of M10 bolts by referring to the study of Muftah et al. [18]. Every built-up CFS channel section has two bolts and nuts.

Table 2 The description and symbols of the specimen

Symbols	Description	Length	Width	Height
60WOOSB	CFS channel section without OSB	600 mm	50 mm	100 mm
C60WOSB	CFS channel section with OSB	600 mm	50 mm	100 mm
BF60WOSB	Built-up face-to-face CFS with OSB	600 mm	100 mm	100 mm
BB60WOSB	Built-up back-to-back CFS with OSB	600 mm	100 mm	100 mm
40WOOSB	CFS channel section without OSB	400 mm	50 mm	100 mm
C40WOSB	CFS channel section with OSB	400 mm	50 mm	100 mm
BF40WOSB	Built-up face-to-face CFS with OSB	400 mm	100 mm	100 mm
BB40WOSB	Built-up back-to-back CFS with OSB	400 mm	100 mm	100 mm

OSB is used for protecting the CFS section to fail at the initial or beginning of the applied load. The CFS channel section uses timber adhesive to attach with OSB at the flange and web element. The built-up CFS section is using bolt and nut to attach with OSB at the flange element, and timber adhesive to attach with OSB at the flange and web element. Between OSB to OSB is fastened by using timber adhesive. The CFS channel section is proposed for checking the flexural behavior of the specimen without using bolts and nuts. Fig. 5 shows the schematic diagram of the CFS channel section without OSB or specimen of 40WOOSB in the front and side view.

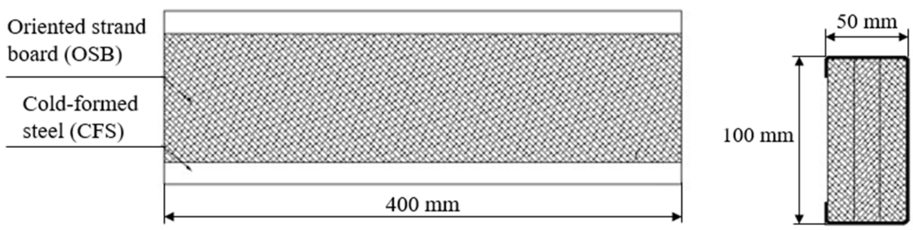

(a) Front view (b) Side view

Fig. 5 The example of the schematic diagram of the 40WOOSB specimen

3.2. Experimental setup

There are three parts of experimental activity in determining the material properties of CFS and OSB, and the flexural behavior of CFS with OSB. The material properties of CFS and physical and mechanical properties of OSB have used the universal testing machine (UTM) with 100 kN of capacity and the flexural behavior is utilized through the flexural machine with 100 kN of capacity which is attached to a compressive strength machine. The pacing rate of 0.5 mm/min is considered for testing of material properties of CFS, and the physical and mechanical properties of OSB. Whereas, the pacing rate of 0.02 kN/s is utilized for flexural behavior testing. An example of the physical and mechanical properties test diagram specifically MOR, MOE, and internal bonding is shown in Fig. 6.

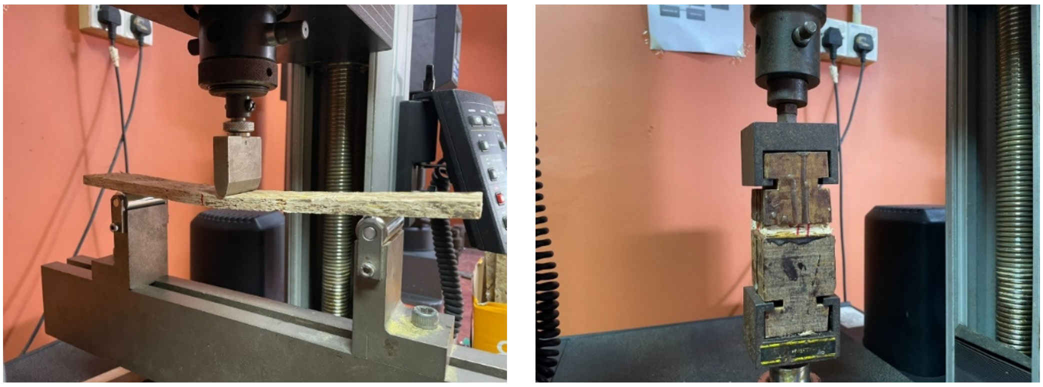

(a) MOR and MOE test (b) Internal bonding test

Fig. 6 The schematic diagram of the physical and mechanical properties test

The chemical properties of the CFS are by using a glow discharge spectrometer testing to determine the quality and authenticity of the steel material used. Tensile testing with the UTM is used to assess the mechanical behavior of the bolt and nut for the built-up CFS section. The three-point flexural test is conducted as shown in Fig. 7. As mentioned before, there are two specimens with a difference in length of the specimen which is noted to be 400 mm and 600 mm. The length of support-to-support of 400 mm and 600 mm is 250 mm and 450 mm, respectively.

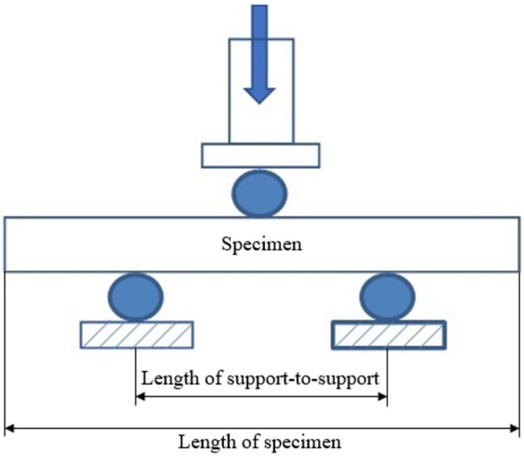

Fig. 7 The schematic diagram of the flexural behavior test

4. Result and Discussion

The result and discussion of material properties of CFS, physical and mechanical properties of OSB, and flexural behavior of CFS with OSB are analyzed and discussed here. Besides, the failure shape of the specimens is also discussed and the result data of experimental activity is compared with previous studies.

4.1. Material properties of CFS

The result of the material properties of CFS is tabulated in Table 3. Fig. 8 shows the load versus deformation and stress versus strain of the coupon specimen. The bending and curving procedure naturally caused the flange element to have a larger yield and ultimate strength rather than the web element. The ultimate load and deformation differences between the web and flange elements are about 0.63 % and 33.50 %, respectively. When an element is bent and shaped from a flat condition to other curved shapes, the ultimate load is what determines how much pressure is placed on it. With cold-forming and a resulting decrease in ductility, the element's ultimate strength is enhanced. For example, on the issue, the web element as a flat condition could be bent either in the right or left position to produce a flange element. The additional strength is occurred and is added to existing strength when the process of bending took place. Hence, the ultimate load of the flange element is more than the web element due to additional strength within the process of bending and shaping the element.

Table 3 The material properties of CFS

Element	Ultimate load (kN)	Deformation at ultimate load (mm)	Ultimate tensile strength, f_u (MPa)	Yield strength, f_y (MPa)	Deformation at yield load (mm)	Modulus of elasticity (GPa)	Factory yield strength, f_{yf} (MPa)	f_u / f_y
Web	4.093	1.05847	511.732	487.997	0.50062	216.45	450	1.049
Flange	4.119	1.59175	514.973	506.110	0.88474	200.18	450	1.018

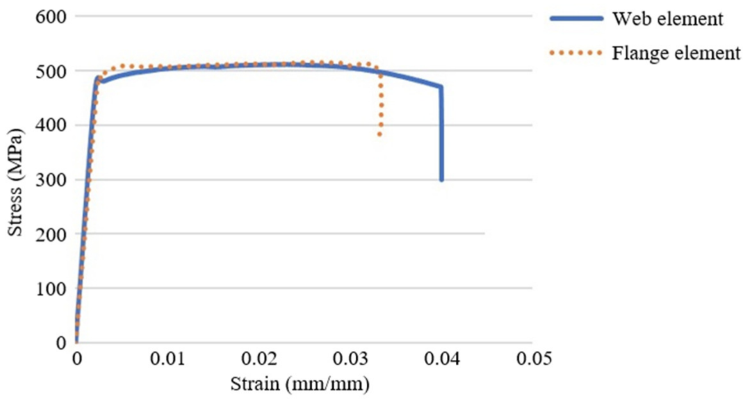

Fig. 8 The graph of the stress versus strain of CFS

The f_u / f_y ratio is a factor that determines how cold work conditions affect mechanical qualities. According to the result data, the ratio of f_u / f_y and f_u / f_{yf} for the web element is 1.049 and 1.137, respectively. Furthermore, the ratio of f_u / f_y and f_u / f_{yf} for the flange element is reported to obtain 1.018 and 1.144, respectively. The values of f_u / f_y of the web and flange element are reported to be significantly larger than 1.10 and recognized as good material in ductility when referring to BS EN 1993-1-1 [15]. To prevent brittle fracture of the steel material in structures, ductility is crucial.

Table 4 The chemical properties of CFS

Chemical composition	Value (%)		
	CFS channel section	CFS G450 Pham et al. [19]	CFS G550 Chen et al. [20]
Iron (Fe)	99.0	97.52 - 99.70	99.57
Carbon (C)	0.0505	0.035 - 0.07	0.036
Manganese (Mn)	0.175	0.2 - 0.3	0.212
Phosphorus (P)	0.0309	0.00 - 0.02	0.020
Sulphur (S)	0.00848	0.00 - 0.02	0.011
Nickel (Ni)	0.314	-	0.038
Zirconium (Zr)	0.178	-	-
Silicon (Si)	0.0145	0.00 - 0.02	0.062
Titanium (Ti)	0.0274	-	-
Aluminium (Al)	0.0182	0.02 - 0.07	-
Chromium (Cr)	0.0213	-	0.056

The chemical properties of the CFS channel section are tested and the result of the testing is tabulated in Table 4. It showed that the CFS channel section that is used contributed 99.0 % for iron in the total amount of chemical composition. Thus, the specimen is classified as a purely steel-based material. The composition of nickel in the CFS channel section with the second highest amount could help the improvement of the fracture toughness and corrosion resistance. The percentage amount of Phosphorus in the CFS channel section is not too high because the role of existing it will reduce the ductility of the material. The material has a carbon concentration of 0.0505 %, which is vital for producing the material's strength. The chemical composition of CFS material is compared with the CFS grade G450 and G550 that were used by Pham et al. [19] and Chen et al. [20] in their research, respectively. The amount of iron in the specimens varies by roughly 0.57 % between CFS and CFS G550. The amount of Manganese between all CFS specimens is close to each other.

The mechanical behavior of the bolt and nut is conducted and the result is discussed here. The ultimate load and tensile strength of the bolt are 30.24 kN and 385.09 MPa, respectively. The deformation of the bolt at ultimate load condition is reported as having 2.97815 mm. The graph of the load versus deformation of the bolt and nut is illustrated in Fig. 9.

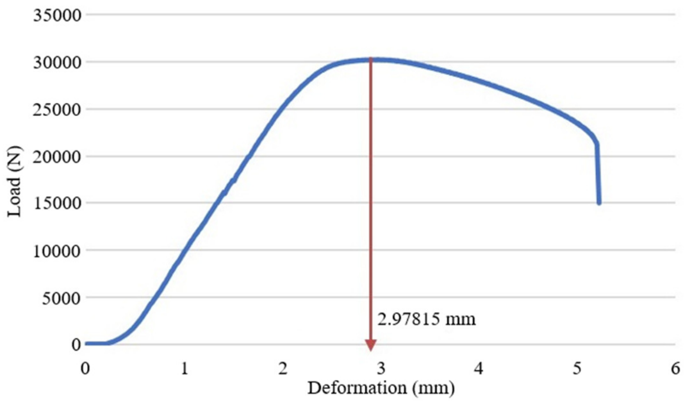

Fig. 9 The load versus deformation graph for bolt and nut

4.2. *Physical and mechanical properties of OSB*

Before being utilized for attaching to the CFS channel and built-up CFS section, the material properties of OSB include the primary strength values that assessed their structural integrity, such as MOR and MOE. Additionally, the internal bonding and thickness swelling is tabulated in Table 5.

Table 5 The physical and mechanical properties of OSB

	This study	Christoforo et al. [21]
	Species	
	Poplar, Combi, Pine, or Hardwood	Schizolobium amazonicum
Properties	Value	
Modulus of rupture (MOR)	17.54 MPa	49.51 MPa
Modulus of elasticity (MOE)	2969 MPa	6084 MPa
Density	702.3 kg/m^3	630 kg/m^3
Internal bonding	248 MPa	0.54 MPa
Thickness swelling	57.03 %	20.41 %
Water absorption	10.87 %	54.94 %

The physical and mechanical of the selected OSB are compared with other species of wood which are studied by Christoforo et al. [21]. The percentage difference of the MOR and MOE between selected OSB and the study by Christoforo et al. [21] is 64.57 % and 51.20 %, respectively. Lopes et al. [22] reported that the minimum value of MOE and MOR in American National Standards Institute (ANSI) 208.1 is 1725 MPa and 11.33 MPa. Thus, the selected OSB stated that the value of MOE and MOR met the requirement of ANSI 208.1. The density of both OSB specimens is below 800 kg/m^3 and similar to the study by Lopes et al. [22] which mentioned the density of the OSB with different materials in the range of 640 kg/m^3 to 1020 kg/m^3. The water absorption of the selected OSB is classified to have good water resistance when compared with the previous study. From the testing, the physical and mechanical properties of selected OSB are not as good as the timber species in the study by Christoforo et al. [21] but are appropriate when attached to a main structure such as steel-based material.

4.3. Flexural behavior of built-up cold-formed steel channel section strengthened with oriented strand board

The complete result of the flexural behavior test is shown in Table 6 including the mass, flexural strength, and failure mode. The heavier specimen among all specimens is built-up CFS with OSB in face-to-face configuration. The mass of the CFS channel section is increased when the OSB is attached with OSB with approximately 36.72 % for a length of 400 mm and 37.10 % for a length of 600 mm. 69.90 % and 69.69 % recorded when the mass of 400 mm length of the CFS channel section without OSB compared with the built-up CFS with OSB in face-to-face and back-to-back configuration, respectively. Whereas the percentage difference of the mass of 600 mm length of the CFS channel section without OSB with the built-up CFS with OSB in face-to-face configuration is 70.65 % and in back-to-back configuration is 69.15 %. Lastly, for lengths of 400 mm and 600 mm, the mass difference between the built-up CFS with OSB in face-to-face and back-to-back configurations are 0.73 % and 4.89 %, respectively.

Table 6 The flexural behavior of the built-up CFS channel section

Specimen	Mass (kg)	Ultimate load (kN)	Flexural strength (MPa)	Failure mode
40WOOSB	1.0521	11.43	21.95	Local, distortional, and global buckling
C40WOSB	1.6625	15.87	11.90	Local and distortional buckling
BF40WOSB	3.4965	59.43	22.29	Local buckling
BB40WOSB	3.4710	73.10	27.41	Local buckling
60WOOSB	1.5829	7.38	25.51	Local, distortional, and global buckling
C60WOSB	2.5165	21.26	28.71	Local and distortional buckling
BF60WOSB	5.3940	37.16	25.08	Local buckling
BB60WOSB	5.1305	45.98	31.04	Local buckling

The mass of the specimen is not influenced directly by the result of the ultimate load and flexural strength but the aspect that inclined to them is a cross-section, dimension, and section properties of the web and flange element in this experiment. As observed from the result of the specimen BF40WOSB and BF60WOSB is heavy when compared with BB40WOSB and BB60WOSB but the result of the ultimate load is low when compared to both specimens. Fig. 10 illustrates the relationship between the mass of the specimen with the type of specimens in varying lengths.

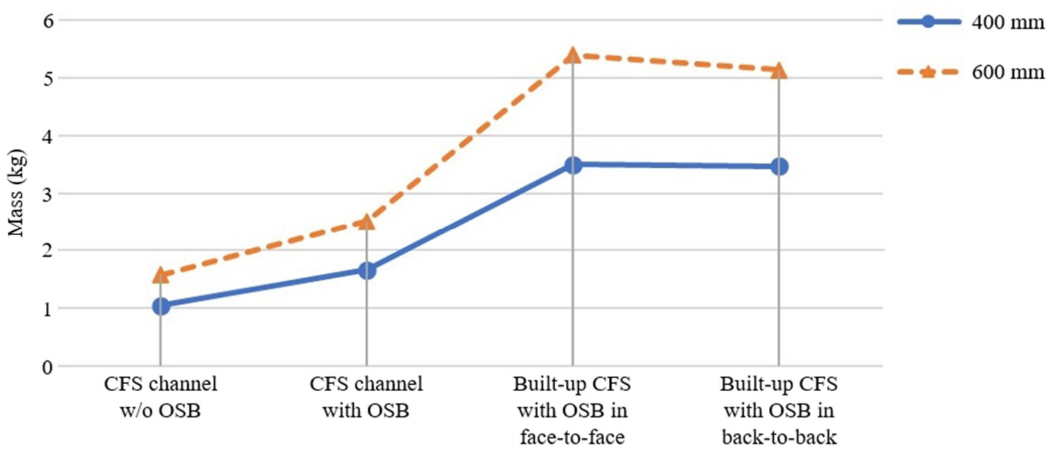

Fig. 10 The mass of the different types of specimens with varying length

The ultimate load of the beam is increased when the length of the beam decreased as shown in Fig. 11. The built-up CFS with OSB in back-to-back configuration is noted to have the highest ultimate load when compared with the built-up CFS with OSB in face-to-face configuration. 18.70 % and 19.18 % percentage differences of the ultimate load are reported when comparing BF40WOSB with BB40WOSB and BF60WOSB with BB60WOSB, respectively. This is because the height of the beam with a thicker element of the section for example the web element of the built-up CFS with OSB in back-to-back configuration helped to prevent the local and distortional buckling when the load is applied.

The web element of the beam in face-to-face configuration is 1.55 mm in two directions and the web element of the beam in back-to-back configuration is twice 1.55 mm with a total of 3.10 mm. Although the beam in face-to-face configuration is reported to have two directions of steel surface such as of the fully enclosed cage with a void in the middle room is still not able to resist the failure of buckling. From the result, the percentage difference of the ultimate load of the 40WOOSB with C40WOSB is 27.98 % and 60WOOSB with C60WOSB is 65.29 %. The CFS channel section without OSB is classified as flexible circumstances and unstable conditions when subjected to load.

The CFS channel section failed due to local and distortional buckling because they are in open-section and unsymmetrical condition and finally they turned back to the original shape same as before testing. OSB helped the CFS channel section to avoid an unstable condition of the section and reduce the failure of the buckling. The comparison percentage of the ultimate load of the CFS channel section without OSB with the built-up CFS with OSB in face-to-face configuration for 400 mm and 600 mm length is 80.77 % and 80.14 %, respectively. From the percentage difference, it was found that the improvement of the ultimate load of the built-up CFS with OSB in face-to-face configuration is similar for the two different lengths. Therefore, the improvement in the ultimate load of the built-up CFS with OSB in face-to-face configuration is not affected by the length of the beam. Furthermore, the percentage of the comparison between the 40WOOSB with BB40WOSB is 84.36% and 60WOOSB with BB40WOSB is 83.95 %. This statement proves that the improvement of the section even formed in different configurations still obtains the same percentage in different lengths.

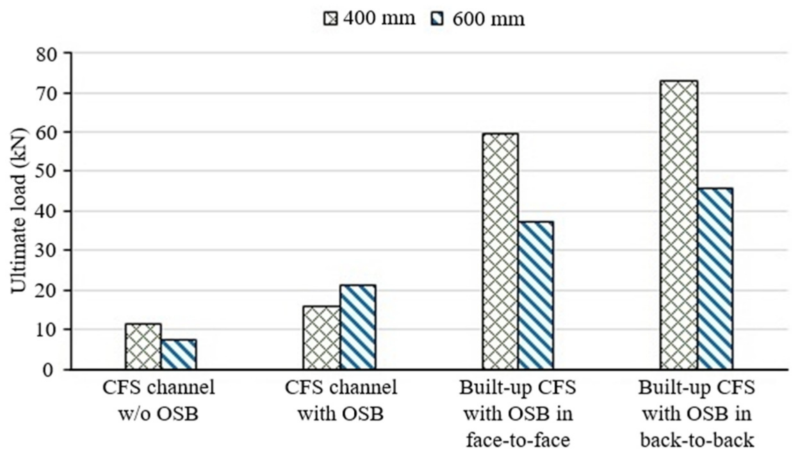

Fig. 11 The ultimate load of the specimens with two different lengths

The failure mode of all specimens is shown in Fig. 12. Fig. 12 also illustrated the schematic diagram before and after the flexural behavior test and the red circle is shown the failure mode after being tested. All specimens are reported to have local buckling and certain specimens are noted to have a combination of local and distortional buckling such as specimens which not in the built-up CFS section. The attachment of CFS and OSB by using timber adhesive is observed to have lost their structural integrity, especially at the top part of the specimen or near the loading for all specimens. The attachment between OSB with other OSB is shown without any failure clearly and visibly, and proves the significance of the use of timber adhesive between them. However, the bolts and nuts are observed not to have any structural integrity issues and remain in the position with no deformation or failure. The contact between the CFS channel section with other channel sections for built-up CFS with OSB whether in back-to-back or face-to-face configuration is reported as not dramatically showing any failure.

The end and middle bolt spacing of 400 mm and 600 mm built-up CFS specimen is shown to have suitability in creating a built-up CFS section and did not affect the flexural behavior. Built-up CFS with OSB either in face-to-face or back-to-back configuration is reported to have the reduction of local buckling and deduction of distortional buckling. The maximum deformation of BF40WOSB is 7 mm and BB40WOSB is 5 mm. In addition, the maximum deformation of BF60WOSB is 39 mm and BB60WOSB is 57 mm. Abou-Rayan et al. [13] have reported that the failure mode of CFS I-beam strengthened hollow flanges is observed to fail inward, local buckling of the flange element at the middle span and no buckling failure at the web element but the outward local buckling of the flange element at loading position is detected for CFS I-beam strengthened hollow flanges with particleboard. The failure of the BB60WOSB and BB40WOSB is similar to the study of Sheta et al. [14] for built-up CFS back-to-back sections with engineered cementitious composites.

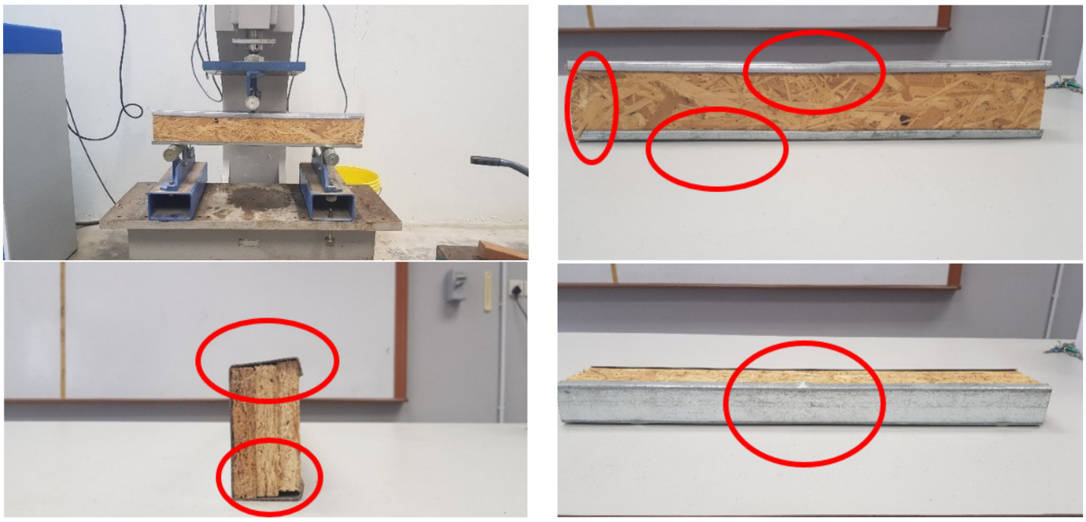

(a) C60WOSB

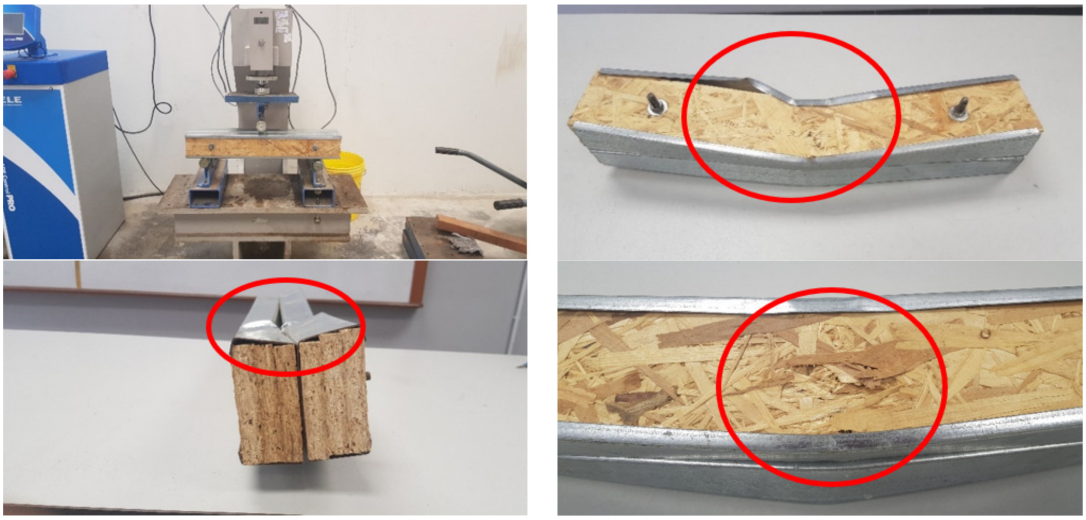

(b) BF60WOSB

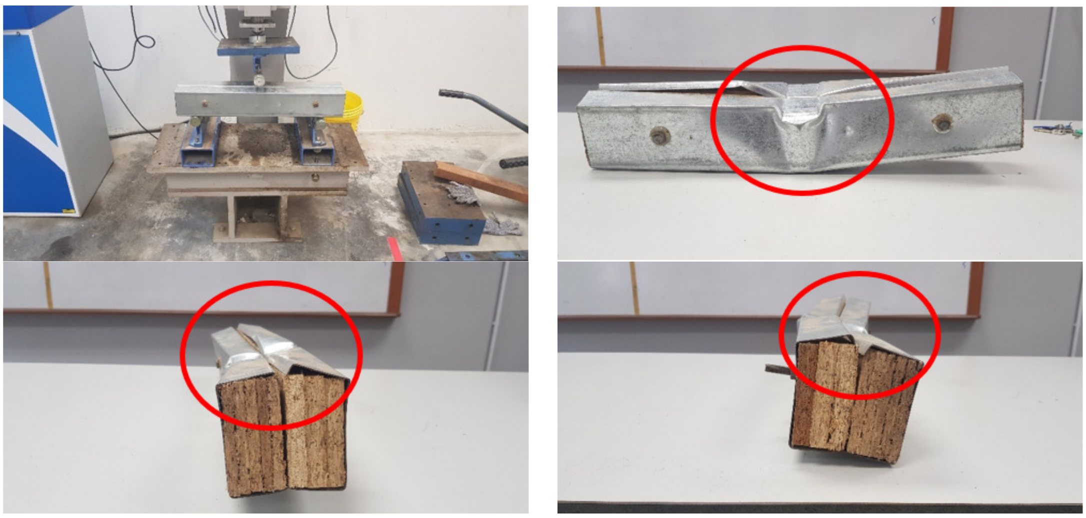

(c) BB60WOSB

Fig. 12 The schematic diagram of the specimen before and after testing

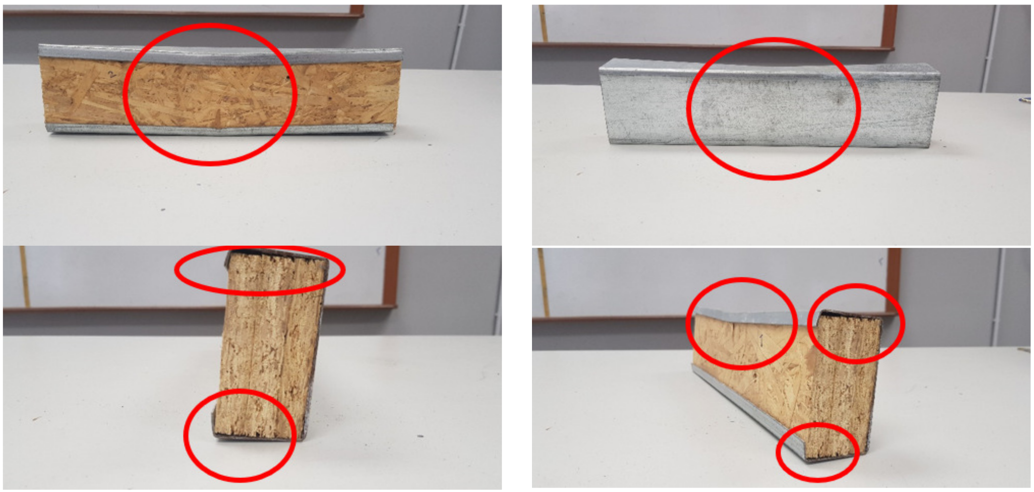

(d) C40WOSB

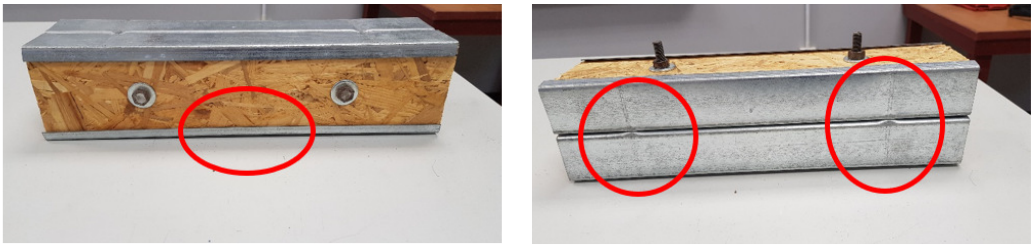

(e) BF40WOSB

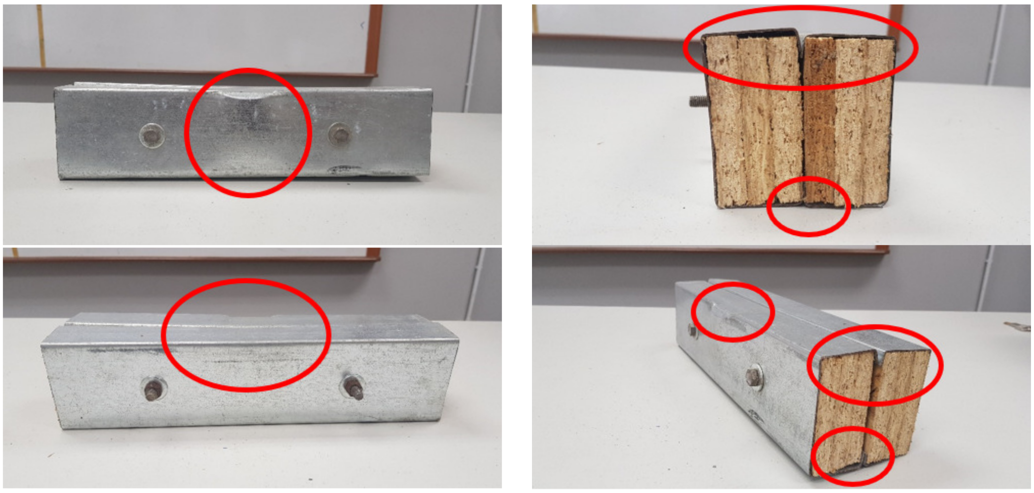

(f) BB40WOSB

Fig. 12 The schematic diagram of the specimen before and after testing (continued)

The OSB which is fastened with the CFS section in the channel section is categorized as partial composite action and the built-up CFS section either face-to-face or back-to-back configuration is classed as full composite action due to the failure mode of the specimens. This is because the built-up CFS with OSB is fastened by a bolt and a nut is more stiffened and avoids the shear failure of the beam.

Rasmussen et al. [23] have mentioned about the two sections if joined together throughout their whole length by a fastener, the abutting surfaces of the web element will be subjected to the same deformation and the full composite action will be obtained. They also stated that in the majority of fastener types, the component of the composite section experienced relative shear deformation at the fastener locations and generated the shear stresses in the fasteners. Thus, the built-up CFS with OSB is reported to have the highest value of ultimate load when compared with the CFS channel section with OSB. If the result of the specimen is compared with the previous study by Sani et al. [24], the percentage difference of ultimate load with BB60WOSB is 80.89 %. The specimen used in the previous study is a built-up CFS face-to-face filled with normal concrete with 900 mm of length, 150 mm of end, and 300 mm of central bolt and nut spacing.

5. Conclusion and Recommendation

In this study, the analysis of the flexural behavior of built-up CFS channel section strengthened with OSB is conducted and supported with the result of the material and chemical properties of CFS, physical and mechanical properties of OSB and mechanical properties of built-up CFS strengthened with OSB is obtained. Moreover, the failure mode of all specimens is observed. Several conclusions and recommendations are made from the analysis of the entire three parts of the experimental activity and the result data, as displayed here.

(1) The material properties of CFS are appropriate for further action and followed the factory data given. The ultimate load of the flange element is higher than the web element due to the additional strength of the bending process and the percentage difference is a note of 0.63 %. The calculation of the ratio of f_u / f_y classified the CFS material as good in ductility. Besides, the chemical properties result showed that the CFS material is purely produced by using steel-based material with 99 % iron.

(2) The physical and mechanical properties of OSB illustrated that the OSB followed the quality and structural integrity introduced by the factory. The selected OSB is not as good as the previous study which used a good-quality wood species.

(3) The highest value of the ultimate load is observed and recognized as a specimen of BB40WOSB and recorded at 18.70 % when compared with BF40WOSB. BB40WOSB is lighter when distinguishing with BF40WOSB specimen. The ultimate load of the specimens is decreased when the length of the beam increased. OSB is suitable for use in filling the gap of the CFS channel section and built-up CFS section because the failure of buckling could be reduced.

For further study, the length of the beam should be added for more relevance and compared with all specimens by using the slenderness ratio. The experimental activity should be compared with the finite element modeling but a serious approach and study should be focused on to obtain a good and relevant comparison. Besides, the width of the selected OSB in the CFS channel section or built-up CFS section should be determined and analyzed.

Acknowledgment

This research is under financial support from the Universiti Teknologi MARA (UiTM) Cawangan Pahang under the Dana Lestari Khas Fasa 3 – 600-TNCPI 5/3/DDN (06) (016/2021). Laboratory equipment and technical supports from UiTM staff of the School of Civil Engineering, College of Engineering of UiTM Cawangan Pahang are also gratefully acknowledged.

Conflicts of Interest

The authors declare no conflict of interest.

References

[1] M. S. H. M. Sani, F. Muftah, N. M. Mohsan, and B. Kado, "Behaviour of Built-Up Cold-Formed Steel Stub Columns Infilled with Washed Bottom Ash Concrete," Advances in Technology Innovation, vol. 7, no. 2, pp. 92-104, April 2022.

[2] S. Selvaraj and M. Madhavan, "Design of Cold-Formed Steel Back-To-Back Connected Built-Up Beams," Journal of Constructional Steel Research, vol. 181, article no. 106623, June 2021.

[3] M. A. Dar, N. Subramanian, A. F. Ghowsi, M. Anbarasu, I. Hajirasouliha, S. Haris, et al., "Intermittently Stiffened Cold-Formed Steel GFRP Composite Lightweight Built-Up Beams: Experimental Investigation and Performance Assessment," Thin-Walled Structures, vol. 185, article no. 110630, April 2023.

[4] A. Guzman, O. Guzman, C. Arteta, and J. Carrillo, "Experimental Study of the Influence of Welding Space in Cold-Formed Built-Up Box Flexural Members," Engineering Structures, vol. 228, article no. 111541, February 2021.

[5] M. Anbarasu, M. A. Dar, A. F. Ghowsi, and A. R. Dar, "Flexural Behaviour of Cover Plated CFS Built-Up Beams Composed of Lipped Channels: Comparison of Test and Design Strengths," Structures, vol. 30, pp. 294-304, April 2021.

[6] M. Sifan, P. Gatheeshgar, S. Navaratnam, B. Nagaratnam, K. Poologanathan, J. Thamboo, et al., "Flexural Behaviour and Design of Hollow Flange Cold-Formed Steel Beam Filled with Lightweight Normal and Lightweight High Strength Concrete," Journal of Building Engineering, vol. 48, article no. 103878, May 2022.

[7] J. V. F. Dias, H. Carvalho, F. C. Rodrigues, K. A. F. P. Maia, and R. B. Caldas, "Experimental and Numerical Study on CFS Composite Beams with Riveted Shear Connectors," Structures, vol. 33, pp. 737-747, October 2021.

[8] P. Kyvelou, T. P. S. Reynolds, C. T. S. Beckett, and Y. Huang, "Experimental Investigation on Composite Panels of Cold-formed Steel and Timber," Engineering Structures, vol. 247, article no. 113186, November 2021.

[9] N. Vella, L. Gardner, and S. Buhagiar, "Experimental Analysis of Cold-Formed Steel-to-Timber Connections with Inclined Screws," Structures, vol. 24, pp. 890-904, April 2020.

[10] S. Navaratnam, D. W. Small, P. Gatheeshgar, K. Poologanathan, J. Thamboo, C. Higgins, et al., "Development of Cross Laminated Timber-Cold-Formed Steel Composite Beam for Floor System to Sustainable Modular Building Construction," Structures, vol. 32, pp. 681-690, August 2021.

[11] A. Awaludin, K. Rachmawati, M. Aryati, and A. D. Danastri, "Development of Cold-Formed Steel-Timber Composite for Roof Structures: Compression Members," Procedia Engineering, vol. 125, pp. 850-856, 2015.

[12] I. S. Irawati, A. Awaludin, and N. P. Sebastian, "The Performance of Cold-formed Steel Long-Span Roof Structure Combined with Laminated Timber: Cold-Formed Steel-Laminated Timber Composite," Procedia Engineering, vol. 171, pp. 1242-1249, 2017.

[13] A. M. Abou-Rayan, N. N. Khalil, and A. A. Zaky, "Experimental Investigation on the Flexural Behavior of Steel Cold-Formed I-Beam with Strengthened Hollow Tubular Flanges," Thin-Walled Structures, vol. 155, article no. 106971, October 2020.

[14] A. Sheta, X. Ma, Y. Zhuge, M. ElGawady, J. Mills, and E. Abd-Elaal, "Flexural Strength of Innovative Thin-Walled Composite Cold-Formed Steel/ PE-ECC Beams," Engineering Structures, vol. 267, article no. 114675, September 2022.

[15] Eurocode 3: Design of Steel Structures - Part 1-1: General Rules and Rules for Buildings, European Standard EN 1993-1-1, 2005.

[16] N. D. Kankanamge and M. Mahendran, "Behaviour and Design of Cold-Formed Steel Beams Subject to Lateral-Torsional Buckling," Thin-Walled Structures, vol. 51, pp. 25-38, February 2012.

[17] Metallic Materials - Tensile Testing - Part 1: Method of Test at Ambient Temperature, European Standard EN 10002-1, 2001.

[18] F. Muftah, M. S. H. Mohd Sani, and M. M. Mohd Kamal, "Flexural Strength Behaviour of Bolted Built-Up Cold-Formed Steel Beam with Outstand and Extended Stiffener," International Journal of Steel Structures, vol. 19, no. 3, pp. 719-732, June 2019.

[19] C. H. Pham, H. N. Trinh, and G. Proust, "Effect of Manufacturing Process on Microstructures and Mechanical Properties, and Design of Cold-Formed G450 Steel Channels," Thin-Walled Structures, vol. 162, article no. 107620, May 2021.

[20] W. Chen, K. Liu, J. Ye, J. Jiang, C. Xu, L. Jin, et al., "High-Temperature Steady-State Experiments on G550 Cold-Formed Steel During Heating and Cooling Stages," Thin-Walled Structures, vol. 151, article no. 106760, June 2020.

[21] A. L. Christoforo, F. S. Ferro, F. N. Arroyo, V. A. Araujo, F. H. Icimoto, H. F. Santos, et al., "Chromated Copper Borate Influence on Physical and Mechanical Properties of Oriented Strand Boards Using Schizolobium Amazonicum Wood Specie," Construction and Building Materials, vol. 356, article no. 129237, November 2022.

[22] M. D. M. Lopes, M. D. S. Padua, J. P. R. G. D. Carvalho, N. T. Simonassi, F. P. D. Lopez, H. A. Colorado, et al., "Natural Based Polyurethane Matrix Composites Reinforced with Bamboo Fiber Waste for Use as Oriented Strand Board," Journal of Materials Research and Technology, vol. 12, pp. 2317-2324, May-June 2021.

[23] K. J. R. Rasmussen, M. Khezri, B. W. Schafer, and H. Zhang, "The Mechanics of Built-Up Cold-Formed Steel Members," Thin-Walled Structures, vol. 154, article no. 106756, September 2020.

[24] M. S. H. M. Sani, F. Muftah, M. F. Muda, and C. S. Tan, "Resistance of Built-Up Cold-Formed Steel Channel Columns Filled with Concrete," Jurnal Teknologi, vol. 78, no. 5-2, pp. 99-104, 2016.